Dispersion diagrams of a water-loaded cylindrical shell obtained from the structural and acoustic responses of the sensor array along the shell

B.K. Jung[1]; J. Ryue[2]; C.S. Hong[3]; W.B. Jeong[1]; K.K. Shin[4]

[1] Pusan National University, South Korea

[2] University of Ulsan, South Korea

[3] Ulsan college, South Korea

[4] Agency for Defense Development, South Korea

ABSTRACT

In order to analyze the vibration and the sound radiation from the waveguide structures, it is important to understand the dispersion relations of the waves sustained in the waveguides. By using the sensor arrays mounted on the surface of the waveguides, these dispersion characteristics would be constructed from the structural and acoustic responses at the sensor locations. In this study, the waveguide finite and boundary element method is adopted to predict the dispersion curves for a water-loaded cylindrical shell. The structural responses and near-field acoustic responses of the shell are used to create the dispersion diagrams and the results are compared. Also the effect of the sensor spacing is examined for the two different spans. It was found from this study that the respective dispersion curves constructed from the structural and acoustic signals are considerably different. Also it was seen that the spatial aliasing takes place in the dispersion diagram as the sensor span grows.

Keywords: Waveguide structure, Waveguide FE/BE, Dispersion diagram
I-INCE Classification of Subjects Number(s): 42
(See . http://www.inceusa.org/links/Subj%20Class%20-%20Formatted.pdf .)

1. INTRODUCTION

It is called waveguide structures which have a constant cross-section, such as beams, plates, pipes, and cylinders. In order to analyze the vibration and sound radiation of these waveguide structures, it is important to understand the dispersion relations of the waves sustained in the waveguides. The dispersion relations of the waves are represented by the dispersion curves. The dispersion curve is the typical index showing the propagation characteristics of elastic waves at specific frequency. In this paper, the waveguide finite element method is used to investigate structural and acoustic responses of the submerged shell(1). The waveguide FE is an efficient method to analysis the wave propagation in waveguide structures, using an assumption that the vibration modes of the cross section of the waveguides are propagating harmonically along the longitudinal direction.

The waveguide FEs are used to represent structures which have constant cross-sections along the longitudinal direction. Thus, it has less degree of freedom and operational time than other 3D domain numerical approaches. This takes advantages in the analysis of the waveguide structures which have arbitrary cross-sections that are not suitable for theoretical analysis(2).

If the waveguide structures are water-loaded in the exterior, it needs additional boundary elements for the fluid part. The waveguide BEs is applied to the 2D cross-section of the structure

[1] only417@hanmail.net
[2] jsryue@ulsan.ac.kr
[3] cshong@uc.ac.kr
[4] kkshin@add.re.kr

similarly to the 2D boundary element but allow the harmonic wave propagation along the longitudinal direction. There are a few previous studies utilizing the waveguide FEs and BEs to analyze the propagating characteristics of the waves in the waveguides. C.-M. Nilsson calculated the sound radiated by rail way and tram rails by using the waveguide BE from the forced vibration responses obtained from the waveguide FE(3). J. Ryue has used coupling equations between the waveguide FEs and BEs to predict the vibration of the water-loaded pipe(4).

In this study, the waveguide FE and BE method is adopted to predict the propagation characteristics of the waves of the water-loaded cylindrical shell. From this method, the dispersion diagrams using spatial structural and near-field acoustic responses are obtained and compared. To understand the effect of array length and sensor pacing on dispersion diagrams, two different array lengths and sensor spacing are examined in the reconstruction of dispersion diagrams.

2. Waveguide FEM/BEM

2.1 Waveguide FEM

The waveguide FE method uses a 2D geometry of the cross section with an assumption that vibration modes are propagating along the longitudinal direction harmonically, that is, $e^{-j\kappa x}$, where x denotes the longitudinal axis, κ is the wavenumber along the x axis. This approach is also called semi-analytical FE (SAFE) because it uses a theoretical solution along the longitudinal direction(5).

In this study, the plate element of waveguide FE is used to model the cylindrical shell. The governing equation for the plate elements of waveguide FE is given by

$$\left[K_4 \frac{\partial^4}{\partial x^4} + K_2 \frac{\partial^2}{\partial x^2} + K_1 \frac{\partial}{\partial x} + K_0 - \omega^2 M \right] u(x, y, z) = 0 \tag{1}$$

where K_4, K_2, K_1 and K_0 is stiffness matrices of the plate element, M is a mass matrix, ω is an angular frequency, $u(x, y, z)$ is a displacement vector of the 2D cross section. This displacement vector is defined by following equation.

$$u(x, y, z) = \tilde{U}(x, y, z) e^{-j\kappa x} \tag{2}$$

where, $\tilde{U}$ denotes the deformation of the cross-section. When Eqn. (2) is substituted into Eqn. (1), the equation of motions of the plate element becomes

$$\left[K_4(-j\kappa)^4 + K_2(-j\kappa)^2 + K_1(-j\kappa) + K_0 - \omega^2 M \right] \tilde{U} = 0 \tag{3}$$

Eqn. (3) is a function of two parameters of the frequency and the wavenumber. So if one of them is given, it can be solved by the eigenvalue analysis. When the wavenumber is given, the equation becomes the eigenvalue problem for the frequency. On the other hand, when the frequency is given, the equation becomes the polynomial eigenvalue problem for the wavenumber.

2.2 Waveguide BEM

In the case of the exterior water-loaded waveguide structure problem, it can analyze the radiation phenomena by using the waveguide BE method. The waveguide BEs which models a 2D geometry of the cross section is similar to the 2D conventional boundary elements, but considers the wave propagation along the longitudinal direction. The fundamental equation of waveguide BE is given by

$$\nabla^2 \Psi + \left(k^2 - \kappa^2 \right) \Psi = 0 \tag{4}$$

where ∇^2 is the operator of 2D Laplace, Ψ is the velocity potential, k is the acoustic wavenumber of external fluid. Here, k is defined by ω / c where c is the wave speed in the fluid. The velocity potential Ψ is the function of normal directional particle velocity v_n and acoustic pressure p and defined by

$$v_n = \frac{\partial \Psi}{\partial n}, \quad p = j\omega\rho_0 \Psi \tag{5}$$

where ρ_0 is the density of the external fluid.

Eqn. (4) has a term of $\left(k^2 - \kappa^2\right)$, which differs from the 2D Helmholtz equation. In the case of $k^2 > \kappa^2$, Eqn. (4) represents waves propagating outwards, on the other hand, the case of $k^2 < \kappa^2$ means near-field waves which decay rapidly along the radial direction.

The boundary condition of the 2D cross section model is defined by following formula.

$$\int_\Gamma \left(\delta\Psi^* \frac{\partial \Psi}{\partial n} - \Psi \frac{\partial(\delta\Psi)}{\partial n} \right) d\Gamma = 0 \tag{6}$$

Here, * denotes complex conjugate and Γ means the circumference of the 2D cross-section. From the Eqns (4) and (6), the governing equation of the waveguide BEs is given by

$$H(\kappa,\omega)\Psi + \frac{G(\kappa,\omega)}{j\omega\rho_0}\frac{\partial \Psi}{\partial n} = 0 \tag{7}$$

where $H(\kappa,\omega)$ and $G(\kappa,\omega)$ is the matrices of the function of wavenumber and frequency

2.3 Coupling of waveguide FE/BE

The governing equation of waveguide structures excited by external forces and fluid loads is given by

$$\left[K(\kappa) - \omega^2 M\right]\tilde{U} - C_1 p - F_e = 0 \tag{8}$$

where F_e is the external force vector and $C_1 p$ is the force from the fluid loading, C_1 is the coupling matrix which defines the coupled dofs between the structure and the fluid. To define the coupling equation, it needs a continuity condition between the waveguide FEs and BEs, given by

$$v_n = j\omega C_2 \tilde{U} \tag{9}$$

where C_2 is the coupling matrix which converts the Cartesian coordinate system to the normal direction system. Eqn. (9) means the normal velocity of the structure is equal to the particle velocity of the boundary of the structure.

From the Eqns. (7)~ (9), the fully coupled equation is defined by

$$\begin{bmatrix} K(\kappa) - \omega^2 M & -C_1 \\ j\omega C_2 G(\kappa,\omega) & H(\kappa,\omega) \end{bmatrix} \begin{Bmatrix} \tilde{U} \\ p \end{Bmatrix} = \begin{Bmatrix} F_e \\ 0 \end{Bmatrix} \tag{10}$$

If the external force in the right-hand side is given, the displacements and pressures on the waveguide are solved.

3. Numerical analysis

In this section, the waveguide FE/BE analysis is performed to obtain the structural and near-field acoustic responses of the water-loaded cylindrical shell. These spatial responses are utilized to estimate the structural and acoustic dispersion diagrams.

3.1 Analysis model

Figure 1 is the numerical analysis model of a water-loaded cylindrical shell. This model consists of plate elements for the structure part (waveguide FE) and 3 noded elements for the external water (waveguide BE). The number of nodes and elements for the waveguide FE are set to 64, respectively, and 128 and 64 for the waveguide BE. Table 1 shows the material properties of the cylindrical shell and the external water.

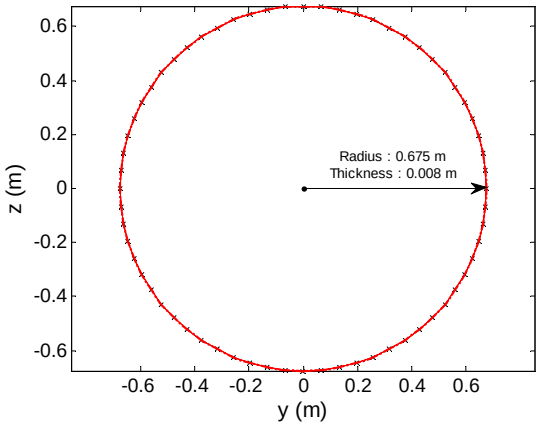

Figure 1 – The waveguide FE/BE model of the cylindrical shell

Table 1 – Material properties

Material	Steel	Material	Water
Elastic modulus, E	200GPa	Wave speed, c	1486
Poisson ratio, ν	0.2792	Density, ρ_0	998
Density, ρ	7900kg/m3		
Damping, η	0.001		

3.2 Wave analysis of the cylindrical shell model

For a unit-force applied, the structural and near-field acoustic responses was calculated by using the coupling equation of the WFE/BE. Figure 2 shows the cross-sectional model with the excitation and response points. Figures 3 and 4 show the spatial structural responses and acoustic pressures at 300Hz and 1500Hz along the cylinder. The origin in x axis represents a point where the excitation is applied.

The dispersion diagrams can be constructed by using the Fourier transform of these spatial structural and acoustic responses. In the wavenumber domain, the responses will have resonance peaks at the wavenumbers of the propagating waves. These peaks appeared distinctively in the dispersion diagrams at specific frequency.

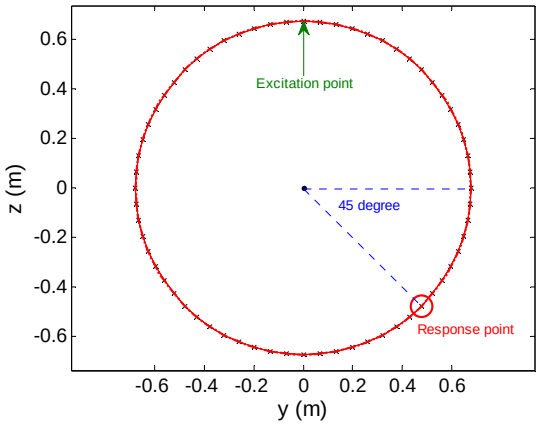

Figure 2 – The excitation and response point of the cylindrical shell

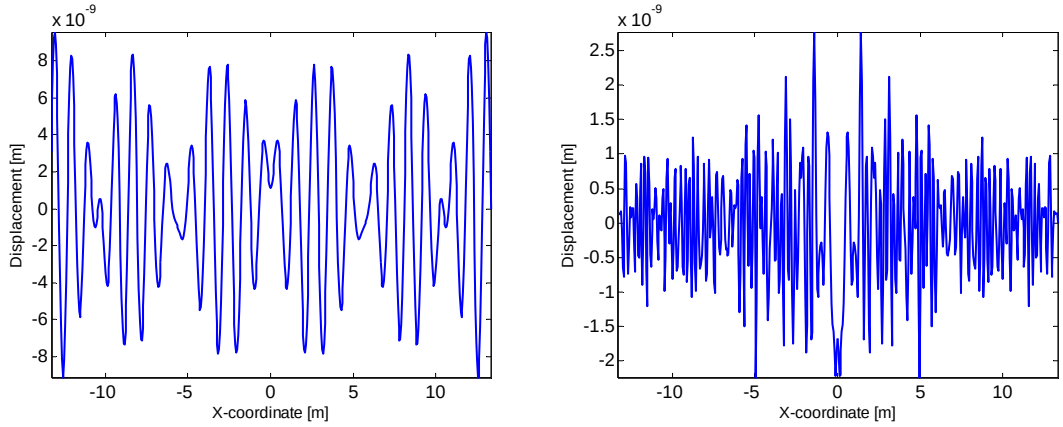

(a) 300 Hz (b) 1500 Hz

Figure 3 – The structural spatial response according to the frequency

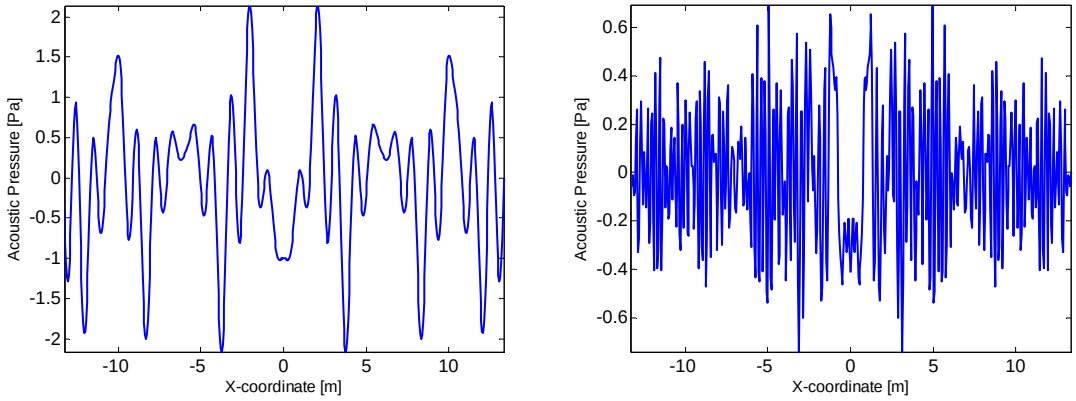

(a) 300 Hz (b) 1500 Hz

Figure 4 – The near-field acoustic spatial response according to the frequency

Figure 5 shows the structural and acoustic dispersion diagrams of the cylindrical shell constructed. In Figure 5, the redder regions represent the stronger responses. The longitudinal and torsional waves are displayed with the straight lines. Because the wave speeds of the longitudinal waves are the faster than those of the torsional waves, the longitudinal wave lines have lower slopes than the torsional waves in the dispersion diagrams. The bending waves are represented with the curved lines

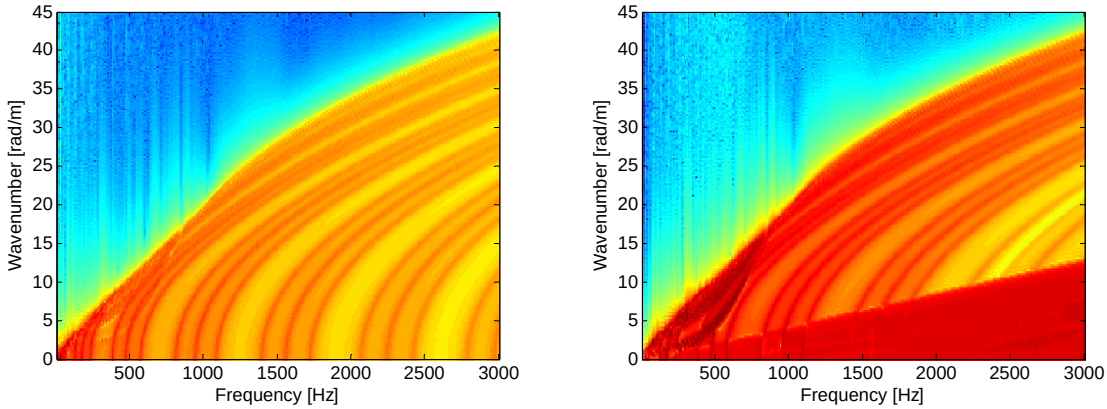

(a) (b)

Figure 5 – The dispersion diagrams of the cylindrical shell produced by (a) structural response, (b) acoustic response.

because they are dispersive.

Since the directions of the excitation and the responses chosen are perpendicular to the circumference of the cylinder, the bending waves appear mainly in the structural dispersion diagram in Figure 5(a). On the other hand, the acoustic dispersion diagram in Figure 5(b) shows the longitudinal, torsional waves additionally, because the acoustic waves are induced by all of these structural vibrations. Especially, the acoustic dispersion diagram shows strong responses in wavenumber regions where the structural wave travels faster than the acoustic wave. It is known that the structural waves of $k < \kappa$ do not radiate well but the dispersion diagram in Figure 5(b) reveals considerably large pressures even in this subsonic ranges. That is because the near-field pressures are used in Figure 5(b), which are calculated on the cylinder surface.

To examine the decaying features of the acoustic signals, the characteristics of the dispersion diagrams are built and compared by increasing the distance between the cylinder and receiving points in water. The distance of the receiving point from the center of the cylindrical shell was set to 1m, 2m and 3m, respectively. Figure 6 shows the acoustic dispersion diagrams according to the distanced of the sensor position from the center of the shell.

Figure 6 shows that the near-field waves disappear rapidly as the distance increases from the center of the cylinder. In the case of the distance of 3m, only the supersonic structural waves, mainly the longitudinal and torsional waves remain, in addition to the free acoustic wave. It is sure that the bending waves hardly contribute to the far field radiation.

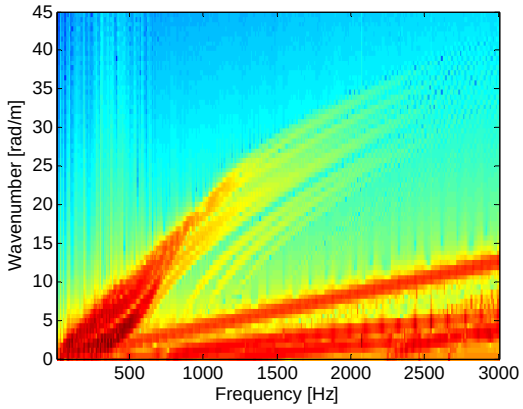

(a) The distance: 1.0 meter

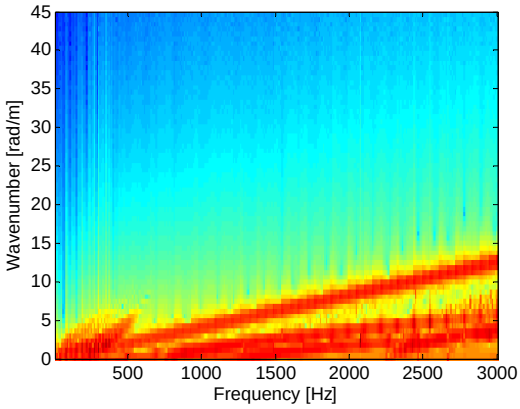

(b) The distance: 2.0 meter

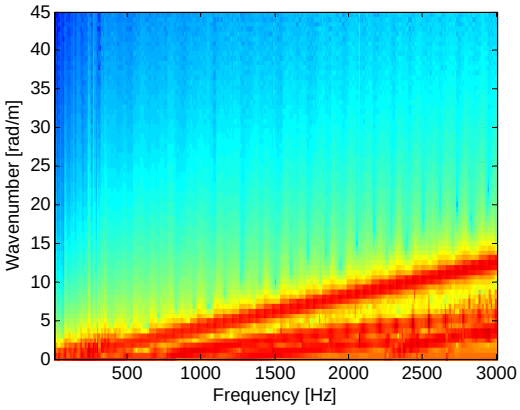

(c) The distance: 3.0 meter

Figure 6 – The acoustic dispersion diagram for various distances between the cylinder and receiving points.

3.3 Estimation of the dispersion diagrams using the responses of array sensors

In this section, the spatial responses at the array sensor positions mounted on the cylinder are used to construct the dispersion diagrams. In terms of the self-noise of the array sensors, the responses at the sensor position are analyzed. To obtain these dispersion diagrams, the sensor array was set to 10m long from the excitation position of x=0. The spans between the two adjacent sensors

are chosen to 0.05m and 0.15m. So the total numbers of sensors for these two cases are 201 and 67, respectively.

Figures 7 and 8 show the spatial structural and acoustic responses of the sensor positions at 300Hz and 1500Hz for the two sensor spans. The spatial responses of 300Hz in Figures 7 and 8 are almost the same despite the different sensor spacing. However, the responses at 1500Hz show aliasing problems when the sensor spacing becomes 0.15m. This aliasing in spatial domain makes

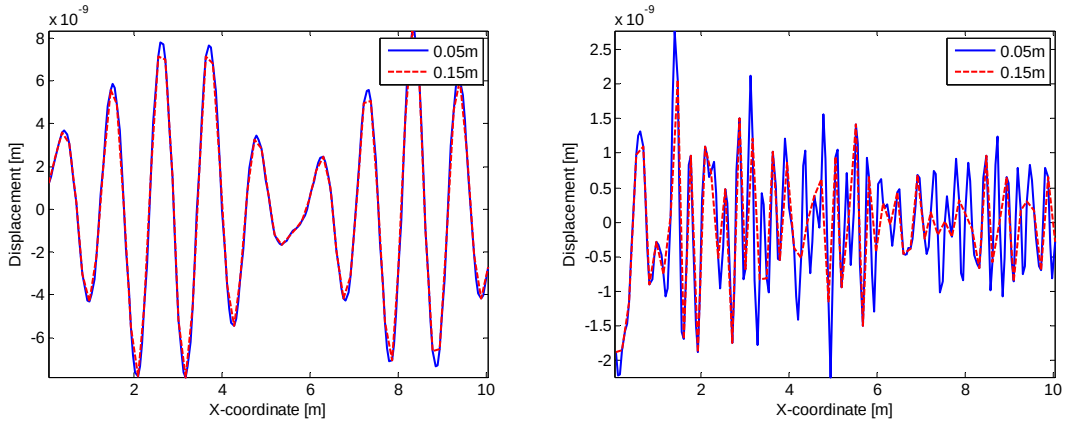

(a) 300 Hz (b) 1500 Hz

Figure 7 – The structural spatial responses of the cylindrical shell for the two different sensor spacing

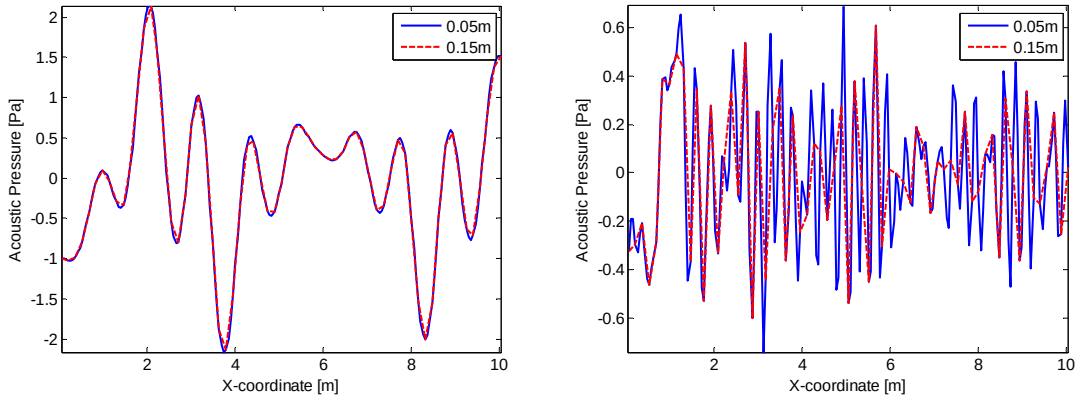

(a) 300 Hz (b) 1500 Hz

Figure 8 – The acoustic spatial responses of the cylindrical shell for the two different sensor spacing

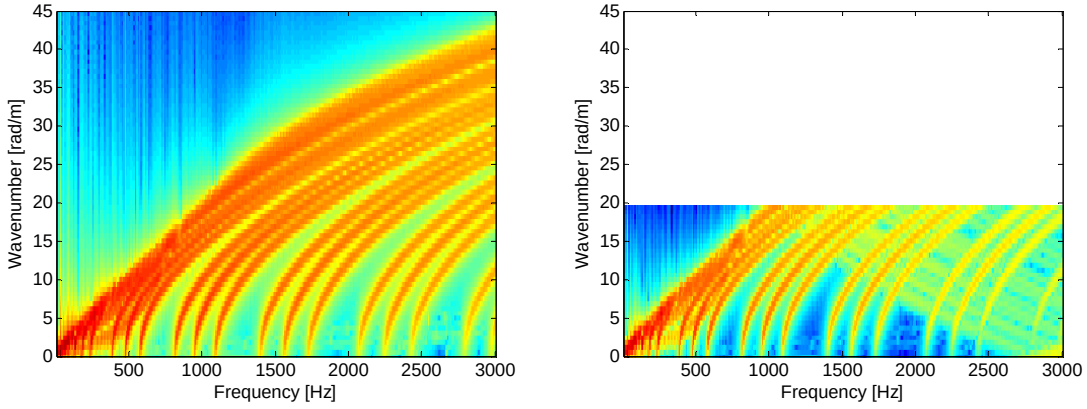

(a) Sensor spacing: 0.05 meter (b) Sensor spacing: 0.15 meter

Figure 9 – The structural dispersion diagrams according to sensor spacing

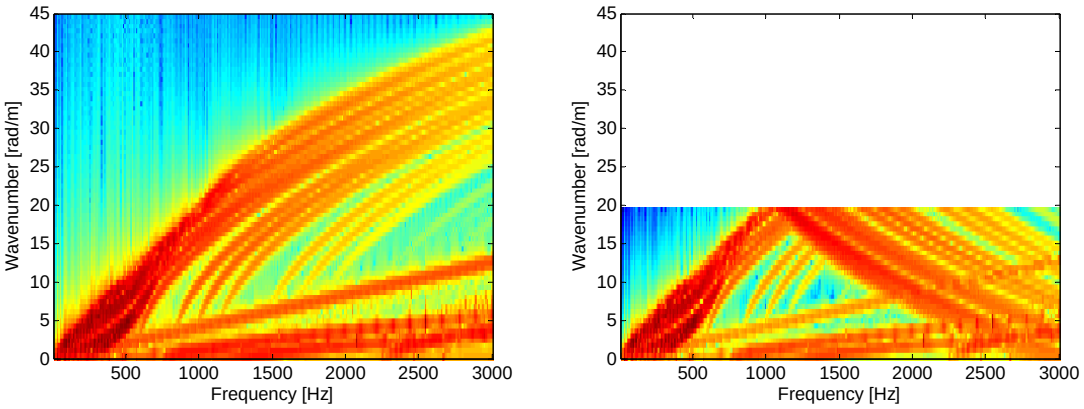

(a) Sensor spacing: 0.05 meter (b) Sensor spacing: 0.15 meter

Figure 10 – The acoustic dispersion diagrams estimated according to sensor spacing

high wavenumber signals to be seen as low wavenumber signals. Therefore, the wavenumber range in dispersion diagrams is bounded to $2\pi/d$, where d is the sensor spacing.

Figures 9 and 10 show the structural and acoustic dispersion diagrams estimated by using the 0.05m and 0.15m sensor spacing. Figures 9(b) and 10(b) reveals the distortion of the dispsersion diagrams caused by the spatial aliasing when the 0.15m sensor spacing is used. This problem appears more distinctively in the acoustic dispersion diagrams.

4. Conclusion

The dispersion diagrams have the information about the dispersion relations of the waves sustained in waveguide structures. In this paper, a numerical analysis method, called the waveguide FE/BE was used to estimate the dispersion diagrams of a water-loaded cylindrical shell to figure out the dispersion characteristic. Two different dispersion diagrams were constructed by using structural and acoustic responses, respectively. Two sensor spacing was regarded to figure out the effect of the distance of sensor spacing. It was found that the respective dispersion diagrams constructed from the structural and acoustic signals are considerably different. It was seen that the near-field waves are strongly contribute to the acoustic dispersion diagram. The aliasing problem takes place in the spatial responses when the sensor spacing grows. This aliasing in spatial domain makes high wavenumber signals to be seen as low wavenumber signals. It may lead to the wrong interpretation of the measured signals by the array sensors. In future works, the dynamic excitation forces generated by the operating machines onboard will be included and examine the structural/acoustic dispersion diagrams to see the effect of the internal structures.

ACKNOWLEDGEMENTS

This study was supported by Agency for Defense Development in Korea.

REFERENCES

1. Finnveden S, Nilsson C M. Input power to waveguides calculated by a finite element method. Journal of sound and vibration. Vol 305; 2007. p. 641-658.
2. Gavris L. Finite element computation of dispersion properties of thin-walled waveguides. Journal of sound and vibration. Vol 173; 1994 p. 113-124.
3. Nilsson C M, Jones C, Thompson D, Ryue J. A waveguide finite element and boundary element approach to calculating the sound radiated by railway and tram rails. Journal of Sound and Vibration. Vol 321. No 3-5; 2009. p. 813-836
4. Ryue J. A numerical method for analysis of the sound and vibration of waveguides coupled with external fluid. The Acoustic Society of Korea. Vol 29. No 7; 2010 p. 448-457
5. Bartoli I, Marzani A, Lanze D, Scalea F, Viola E. Modeling wave propagation in damped waveguides of arbitrary cross-section. Journal of Sound and Vibration. Vol 295. No 4; 2006. p. 685-707.